First Complexes of a 4-Alkyl-3,5-di(2-pyridyl)-4*H*-1,2,4-triazole: Synthesis, X-ray Crystal Structures and Magnetic Properties of Dinuclear Cobalt(II), Nickel(II) and Copper(II) Complexes of 4-Isobutyl-3,5-di(2-pyridyl)-4*H*-1,2,4-triazole

Marco H. Klingele,[a] Peter D. W. Boyd,[b] Boujemaa Moubaraki,[c] Keith S. Murray,[c] and Sally Brooker*[a]

Keywords: 1,2,4-Triazole / Bridging ligands / N ligands / Magnetic properties / X-ray diffraction

The reaction of the new, bis(bidentate), potentially dinucleating ligand 4-isobutyl-3,5-di(2-pyridyl)-4*H*-1,2,4-triazole (ibdpt) with $M(ClO_4)_2{\cdot}6H_2O$ (M = Co^{II}, Ni^{II} or Cu^{II}) in a 1:1 molar ratio in MeCN affords the dinuclear complexes $[Co^{II}_2(ibdpt)_2(MeCN)_2(H_2O)_2](ClO_4)_4$ (**1**), $[Ni^{II}_2(ibdpt)_2(MeCN)_4](ClO_4)_4$ (**2**) and $[Cu^{II}_2(ibdpt)_2(MeCN)_2(ClO_4)_2](ClO_4)_2{\cdot}2MeCN$ (**3**). Complex **1** is obtained as a mixture of the red-orange polymorph **1a** and the yellow-orange polymorph **1b**, the main difference between the two forms being the hydrogen bonding patterns between the H_2O co-ligands and the ClO_4^- counterions. The mononuclear complex $[Cu^{II}(ibdpt)_2(ClO_4)_2]$ (**4**) was initially obtained as a minor by-product in the preparation of complex **3** but can also be deliberately prepared from $Cu(ClO_4)_2{\cdot}6H_2O$ and ibdpt in MeCN using a metal-to-ligand molar ratio of 1:2. All five complexes have been structurally characterised by X-ray diffraction. In the dinuclear complexes **1**–**3** the $(N',N^1,N^2,N'')_2$double bridging coordination mode is realised while the mononuclear complex **4** features the common *trans*-$(N',N^1)_2$ coordination mode. In all cases the metal centres reside in distorted octahedral N_4X_2 coordination spheres with axially bound co-ligands (X = H_2O, MeCN or ClO_4^-). The dinuclear complexes **1**–**3** readily lose solvent when taken out of their mother liquors giving rise to partially desolvated materials. Magnetic studies have been carried out on crystalline samples of the resulting complexes that analysed as $Co^{II}_2(ibdpt)_2(ClO_4)_4(MeCN)(H_2O)$ (**5**), $Ni^{II}_2(ibdpt)_2(ClO_4)_4(MeCN)$ (**6**) and $Cu^{II}_2(ibdpt)_2(ClO_4)_4(MeCN)$ (**7**). It was found that in these complexes the two 1,2,4-triazole bridges facilitate antiferromagnetic coupling between the two metal centres (J = –3.76 cm^{-1}, –13.0 cm^{-1} and –105 cm^{-1}, respectively). The coordination compounds described in this paper are the first to incorporate a 4-alkyl-substituted 3,5-di(2-pyridyl)-4*H*-1,2,4-triazole ligand.

Introduction

The strong current interest in the coordination chemistry of 1,2,4-triazole derivatives[1–3] is mainly due to the fact that their ligand strength is in the right region to give complexes with iron(II) salts that show the spin crossover phenomenon.[4–7] Because of their bistability such coordination compounds have potential applications in nano-technology as switches and memory devices, but also as materials for the construction of displays.[8–12] In order for a bistable molecular system to be used in nano-technology it must, however, fulfil certain requirements.[8,9] Most importantly, the transition between the two detectable states should be complete and abrupt with a relatively large thermal hysteresis, centred near room temperature.[13] Such behaviour is associated with cooperative interactions between the metal centres.[14] In mononuclear complexes cooperativity can be conferred by hydrogen bonding, π–π stacking, solvation and the nature of the counterion. These relatively weak interactions pass on the information from one unit to another that the spin transition is occurring. It has been suggested that more pronounced cooperativity could be achieved by the use of ligands capable of bridging metal centres, thus giving rise to oligo- or polynuclear assemblies rather than mononuclear complexes. The employment of mostly 4-substituted 4*H*-1,2,4-triazoles as bridging ligands has allowed the isolation and investigation of various, mainly tri- and polynuclear, spin crossover systems that show promising properties with regard to the requirements outlined above.[4–7] In light of this, we are particularly interested in the synthesis and study of discrete dinuclear iron(II) complexes.[15,16] As a result of these ongoing studies we were recently able to identify the nature of the [low spin–high spin] species of the doubly 1,2,4-triazole-bridged complex $[Fe^{II}_2(PMAT)_2](BF_4)_4{\cdot}DMF$

[a] Department of Chemistry, University of Otago,
P. O. Box 56, Dunedin, New Zealand
Fax: +64-3-479-7906
E-mail: sbrooker@alkali.otago.ac.nz
[b] Department of Chemistry, The University of Auckland,
Private Bag 92019, Auckland, New Zealand
[c] School of Chemistry, Building 23, Monash University,
Clayton, Victoria 3800, Australia
Supporting information for this article is available on the WWW under http://www.eurjic.org or from the author.

  DOI: 10.1002/ejic.200400780

(PMAT = 4-amino-3,5-bis{[(2-pyridylmethyl)amino]-methyl}-4*H*-1,2,4-triazole) by means of X-ray diffraction[15] and thus to confirm the conclusions drawn by Real, Gütlich and co-workers[17,18] on the basis of magnetic and applied-field Mössbauer data about the pathway of the transition in their two-step spin crossover systems.

Structurally related to the bis(terdentate) ligand PMAT (Figure 1) are the bis(bidentate) 4-substituted 3,5-di(2-pyridyl)-4*H*-1,2,4-triazoles.[2] Within this class of potentially dinucleating ligands only two members, namely 4-amino-3,5-di(2-pyridyl)-4*H*-1,2,4-triazole (NH_2dpt)[19,20] and 3,5-di(2-pyridyl)-4-(1*H*-pyrrol-1-yl)-4*H*-1,2,4-triazole (pldpt)[21–23] (Figure 1), have actually produced dinuclear complexes while no 4-aryl-3,5-di(2-pyridyl)-4*H*-1,2,4-triazoles have ever been reported to do so.[24–29] We therefore hypothesised that the coordination behaviour of these bis(bidentate) ligands, i. e. their ability to bind and bridge two metal centres, is influenced not only by factors such as the reaction stoichiometry and product solubility but also by the electronic effects of the substituent on N^4.[2,22] Given that our goal is the preparation of dinuclear iron(II) complexes, it was desirable to test this hypothesis by investigating the coordination chemistry of the hitherto unknown 4-alkyl-3,5-di(2-pyridyl)-4*H*-1,2,4-triazoles which carry electron-donating substitutents on N^4. We recently succeeded in the synthesis of the first two members of this group, namely 4-methyl-3,5-di(2-pyridyl)-4*H*-1,2,4-triazole (medpt) and 4-isobutyl-3,5-di(2-pyridyl)-4*H*-1,2,4-triazole (ibdpt) (Figure 1).[22,30] In this paper we present the results of our investigation of the dinucleation behaviour of the new ligand ibdpt towards the *d*-block ions cobalt(II), nickel(II) and copper(II).

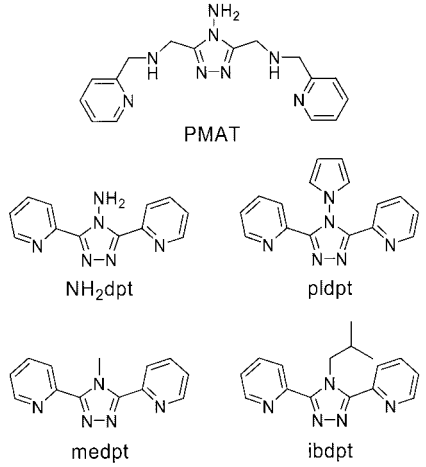

Figure 1. Structural drawings of the ligands 4-amino-3,5-bis{[(2-pyridylmethyl)amino]methyl}-4*H*-1,2,4-triazole (PMAT), 4-amino-3,5-di(2-pyridyl)-4*H*-1,2,4-triazole (NH_2dpt), 3,5-di(2-pyridyl)-4-(1*H*-pyrrol-1-yl)-4*H*-1,2,4-triazole (pldpt), 4-methyl-3,5-di(2-pyridyl)-4*H*-1,2,4-triazole (medpt) and 4-isobutyl-3,5-di(2-pyridyl)-4*H*-1,2,4-triazole (ibdpt).

Results and Discussion

Preparation of the Complexes

The reaction of ibdpt with $M(ClO_4)_2{\cdot}6H_2O$ (M = Co^{II}, Ni^{II} or Cu^{II}) in a 1:1 molar ratio in MeCN produced coloured solutions from which solid products were only obtained upon vapour diffusion of Et_2O. In the case of the cobalt(II) salt this led to the formation of a mixture of red-orange and yellow-orange crystals from the orange reaction mixture in virtually quantitative yield. On the basis of their elemental analyses both crystal types were found to have metal-to-ligand molar ratios of 1:1, not 1:2, and subsequent X-ray diffraction studies showed them to be the two polymorphs **1a** and **1b** of $[Co^{II}_2(ibdpt)_2(MeCN)_2(H_2O)_2](ClO_4)_4$ (**1**). From the purple solution obtained with the nickel(II) salt only one type of purple crystals formed, quantitatively, which were identified by X-ray diffraction as the dinuclear complex $[Ni^{II}_2(ibdpt)_2(MeCN)_4](ClO_4)_4$ (**2**). Using the copper(II) salt instead, blue-green crystals separated from the blue solution which, on prolonged vapour diffusion of Et_2O, were followed by a small amount of steel-blue crystals. Here too, the crystallisation was virtually quantitative. Both crystal types were studied by X-ray diffraction. The blue-green main component was thus identified as the desired dinuclear complex $[Cu^{II}_2(ibdpt)_2(MeCN)_2(ClO_4)_2](ClO_4)_2{\cdot}2MeCN$ (**3**) while the steel-blue minor component was found to be the mononuclear complex $[Cu^{II}(ibdpt)_2(ClO_4)_2]$ (**4**). Complex **4** was readily accessible by the direct reaction of ibdpt with $Cu(ClO_4)_2{\cdot}6H_2O$ in a 2:1 molar ratio in MeCN. Under these conditions it precipitated from the reaction mixture as a blue powder in 48% yield. Vapour diffusion of Et_2O into either the mother liquor or a solution of the powder in MeCN afforded crystals of complex **4** that were identical to those obtained as described above (Table 1).

The dinuclear complexes **1**–**3** readily lost solvent when taken out of their mother liquors. In the case of the yellow-orange polymorph **1b** this was accompanied by a colour change to red-orange while no colour change was observed for the red-orange polymorph **1a**. Subsequent drying of the crystalline samples in vacuo gave rise to partially desolvated materials which were found by elemental analysis to have the compositions $Co^{II}_2(ibdpt)_2(ClO_4)_4(MeCN)(H_2O)$ (**5**) (red-orange), $Ni^{II}_2(ibdpt)_2(ClO_4)_4(MeCN)$ (**6**) (purple) and $Cu^{II}_2(ibdpt)_2(ClO_4)_4(MeCN)$ (**7**) (blue-green). The latter materials were used for further characterisation and magnetic studies.

Description of the Structures

The molecular structures of the red-orange polymorph **1a** (Figure 2) and the yellow-orange polymorph **1b** (Figure S1, Supporting Information) of $[Co^{II}_2(ibdpt)_2(MeCN)_2(H_2O)_2](ClO_4)_4$ (**1**) are very similar, the most obvious difference between them being the orientation of the isobutyl groups of the respective ligand molecule (Figure S2, Supporting Information). The dinuclear $(N',N^1,N^2,N'')_2$ double bridging coordination mode realised in both of these complexes causes distortion of the CoN_5O coordination octahedra and longer Co–N_{pyr} than Co–N_{trz} bond lengths are observed (Table 2 and Table 3). The Co···Co separation in polymorphs **1a** and **1b** are 4.1481(7) and 4.1722(4) Å,

Table 1. Crystallographic data for $[Co^{II}_2(ibdpt)_2(MeCN)_2(H_2O)_2](ClO_4)_4$ (**1**), $[Ni^{II}_2(ibdpt)_2(MeCN)_4](ClO_4)_4$ (**2**), $[Cu^{II}_2(ibdpt)_2(MeCN)_2(ClO_4)_2](ClO_4)_2\cdot 2MeCN$ (**3**) and $[Cu^{II}(ibdpt)_2(ClO_4)_2]$ (**4**).

	1a	**1b**	**2**	**3**	**4**
Empirical formula	$C_{36}H_{44}Cl_4Co_2N_{12}O_{18}$	$C_{36}H_{44}Cl_4Co_2N_{12}O_{18}$	$C_{40}H_{46}Cl_4N_{14}Ni_2O_{16}$	$C_{40}H_{46}Cl_4Cu_2N_{14}O_{16}$	$C_{32}H_{34}Cl_2CuN_{10}O_8$
Formula mass [g mol^{-1}]	1192.49	1192.49	1238.13	1247.79	821.14
Crystal system	monoclinic	monoclinic	monoclinic	triclinic	triclinic
Space group	$P2_1/n$	$P2_1/n$	$C2/c$	$P\bar{1}$	$P\bar{1}$
a [Å]	12.7535(1)	9.0719(1)	12.4932(2)	12.1370(2)	9.2380(5)
b [Å]	13.7125(1)	21.7150(1)	22.3110(1)	13.4873(1)	9.4059(5)
c [Å]	13.6380(2)	12.1300(1)	19.1890(2)	16.3988(1)	10.6591(6)
α [°]	90	90	90	79.678(1)	77.436(1)
β [°]	92.739(1)	99.614(1)	92.612(1)	79.926(1)	81.666(1)
γ [°]	90	90	90	76.488(1)	76.771(1)
V [Å^3]	2382.32(4)	2356.00(3)	5343.1(1)	2542.90(5)	875.59(8)
Z	2	2	4	2	1
$\rho_{calcd.}$ [g cm^{-3}]	1.662	1.681	1.539	1.630	1.557
μ [mm^{-1}]	1.007	1.018	0.983	1.129	0.843
Temperature [K]	83(2)	83(2)	83(2)	83(2)	83(2)
F(000)	1220	1220	2544	1276	423
Crystal colour and shape	red-orange plate	yellow-orange block	purple block	blue-green plate	steel-blue prism
Crystal size [mm^3]	0.20×0.16×0.03	0.40×0.28×0.18	0.42×0.16×0.08	0.24×0.20×0.04	0.35×0.20×0.15
$\Theta_{min.}/\Theta_{max.}$ [°]	2.11/25.69	1.88/25.72	1.83/25.74	1.27/25.68	1.97/25.67
h	–15 → 15	–11 → 10	–15 → 14	–14 → 14	–11 → 11
k	–16 → 6	0 → 26	–27 → 20	–16 → 16	–11 → 11
l	–16 → 15	0 → 14	–20 → 23	–19 → 19	–12 → 12
Reflections collected/R(int)	13076/0.0323	13549/0.0540	15006/0.0352	23025/0.0463	8017/0.0624
Data/restraints/parameter	4504/0/334	4477/0/334	5088/4/395	9523/9/709	3284/0/241
GOF	1.079	1.032	1.047	1.116	1.034
$R1/wR2$ [$I > 2\sigma(I)$]	0.0352/0.0715	0.0254/0.0626	0.0566/0.1543	0.0510/0.1011	0.0494/0.1222
$R1/wR2$ (all data)	0.0509/0.0793	0.0300/0.0647	0.0681/0.1645	0.0773/0.1130	0.0636/0.1313
Max. peak/hole [e·Å^{-3}]	0.344/–0.591	0.382/–0.469	1.606/–0.534	0.584/–0.503	0.647/–0.522

respectively, and thus are somewhat shorter than the corresponding bond length of 4.226(2) Å in $[Co^{II}_2(pldpt)_2(H_2O)_4]Cl_4\cdot 2MeOH\cdot 2H_2O$,[21] the only structurally characterised dinuclear cobalt(II) complex of any 4-substituted 3,5-di(2-pyridyl)-4*H*-1,2,4-triazole previously reported. The torsion angles between the mean planes of the pyridine rings and the central triazole ring in the red-orange polymorph **1a** [8.6(1) and 8.8(1)°] are slightly larger than in the yellow-orange polymorph **1b** [2.3(1) and 8.1(1)°]. In both polymorphs some doming of the ligands is observed. The most significant structural difference between the two polymorphs is found in their hydrogen bonding patterns. In the red-orange polymorph **1a** both ClO_4^- ions form hydrogen bonds to the axial H_2O co-ligand [O(1)···O(11) 2.79 and O(1)···O(21) 2.82 Å] (Figure S3, Supporting Information). In contrast, only one ClO_4^- ion is involved in hydrogen bonding in the yellow-orange polymorph **1b** while the other ClO_4^- ion resides independently within the lattice. A chain of dinuclear units is thus formed with the ClO_4^- ion hydrogen bonding to the H_2O co-ligands of its own and a neighbouring unit in a bridging fashion [O(1)···O(11) 2.76 and O(1)···O(12B) 2.88 Å] (Figure S4, Supporting Information). The shortest bond length between the metal centres of two dinuclear units across this $H_2O\cdots ClO_4^-\cdots H_2O$ link is 8.5770(5) Å while it is only 8.3822(4) Å between the metal centres of two independent chains.

The adoption of the $(N',N^1,N^2,N'')_2$ double bridging coordination mode in $[Ni^{II}_2(ibdpt)_2(MeCN)_4](ClO_4)_4$ (**2**) with MeCN molecules as the axial co-ligands (Figure 3) results in a distorted octahedral N_6 coordination environment about the nickel centres (Table 2 and Table 3). As can be expected for this coordination mode,[2] the Ni–N_{pyr} bond lengths are considerably longer than the Ni–N_{trz} bond lengths [2.139(3)–2.149(3) and 2.023(3)–2.031(3) Å, respectively]. The former are slightly shorter than the corresponding bond lengths observed in $[Ni^{II}_2(NH_2dpt)_2(H_2O)_2Cl_2]Cl_2\cdot 4H_2O$[19] [2.155(1)–2.164(1) Å] while the latter are very similar in both complexes. The Ni···Ni separation in complex **2** is 4.1107(9) Å which is also slightly less than in $[Ni^{II}_2(NH_2dpt)_2(H_2O)_2Cl_2]Cl_2\cdot 4H_2O$ [4.1348(3) Å].[19] The pyridine–triazole–pyridine moiety of the ligand is not completely flat but shows slight doming and torsion angles between the mean planes of the pyridine rings and the central triazole ring of 5.7(2) and 8.7(2)°.

The asymmetric unit of $[Cu^{II}_2(ibdpt)_2(MeCN)_2(ClO_4)_2](ClO_4)_2\cdot 2MeCN$ (**3**) contains two crystallographically independent but structurally very similar complex cations (Table 2 and Table 4), one of which is shown in Figure 4. The Cu···Cu separations in the two cations are 4.0701(10) and 4.0861(9) Å and are thus very similar to one another while they are dramatically shorter than the Cu···Cu separation of 4.415(1) Å found in the only other known dinuclear

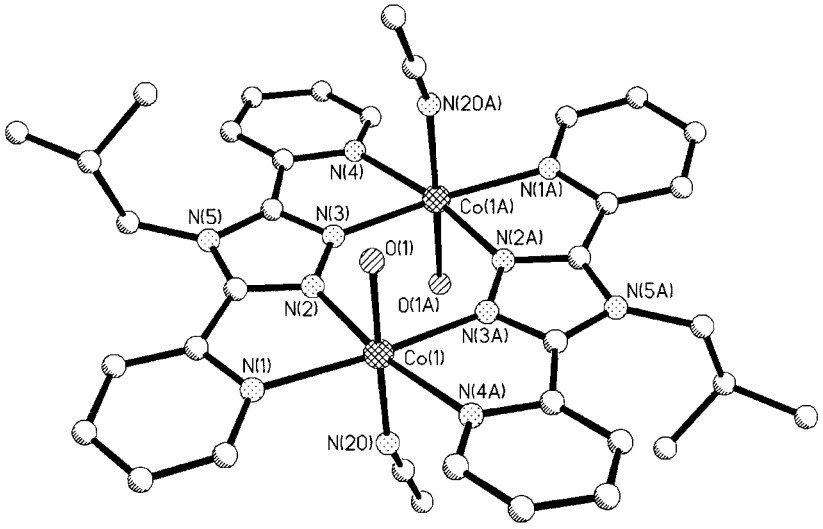

Figure 2. View of the molecular structure of the cation of the red-orange polymorph **1a** of $[Co^{II}_2(ibdpt)_2(MeCN)_2(H_2O)_2](ClO_4)_4$ (**1**). Hydrogen atoms have been omitted for clarity. Symmetry operation used to generate equivalent atoms: (A) $-x, -y, -z + 1$.

Table 2. Selected bond lengths [Å] for $[Co^{II}_2(ibdpt)_2(MeCN)_2(H_2O)_2](ClO_4)_4$ (**1**), $[Ni^{II}_2(ibdpt)_2(MeCN)_4](ClO_4)_4$ (**2**), $[Cu^{II}_2(ibdpt)_2(MeCN)_2(ClO_4)_2](ClO_4)_2 \cdot 2MeCN$ (**3**) and $[Cu^{II}(ibdpt)_2(ClO_4)_2]$ (**4**); values in square brackets refer to the second crystallographically independent complex cation within the asymmetric unit.

	1a	**1b**	**2**	**3**	**4**
M···M	4.1481(7)	4.1722(4)	4.1107(9)	4.0701(10) [4.0861(9)]	
M–N_{pyr}	N(1) 2.185(2)	N(1) 2.1988(14)	N(1) 2.139(3)	N(1) 2.070(3) [N(6) 2.068(3)]	N(1) 2.038(3)
	N(4) 2.164(2)	N(4) 2.1879(14)	N(4) 2.140(3)	N(4) 2.079(3) [N(9) 2.072(3)]	
M–N_{trz}	N(2) 2.069(2)	N(2) 2.0757(14)	N(2) 2.023(3)	N(2) 1.961(3) [N(7) 1.972(3)]	N(2) 1.962(3)
	N(3) 2.083(2)	N(3) 2.0815(14)	N(3) 2.031(3)	N(3) 1.972(3) [N(8) 1.965(3)]	
M–X	N(20) 2.117(2)	N(20) 2.1082(15)	N(20) 2.066(3)	N(50) 2.327(5) [N(60) 2.279(4)]	O(11) 2.471(2)
	O(1) 2.079(2)	O(1) 2.0539(14)	N(30) 2.070(3)	O(11) 2.413(3) [O(21) 2.583(3)]	

Table 3. Selected angles [°] for $[Co^{II}_2(ibdpt)_2(MeCN)_2(H_2O)_2](ClO_4)_4$ (**1**) and $[Ni^{II}_2(ibdpt)_2(MeCN)_4](ClO_4)_4$ (**2**).

1a		**1b**		**2**	
N(1)–Co(1)–N(2)	74.52(8)	N(1)–Co(1)–N(2)	74.46(5)	N(1)–Ni(1)–N(2)	76.61(12)
N(1)–Co(1)–N(3A)	169.33(8)	N(1)–Co(1)–N(3A)	169.14(5)	N(1)–Ni(1)–N(3A)	170.39(12)
N(1)–Co(1)–N(4A)	115.68(8)	N(1)–Co(1)–N(4A)	116.24(5)	N(1)–Ni(1)–N(4A)	113.30(12)
N(1)–Co(1)–N(20)	89.39(8)	N(1)–Co(1)–N(20)	88.61(5)	N(1)–Ni(1)–N(20)	90.02(13)
N(1)–Co(1)–O(1)	91.54(9)	N(1)–Co(1)–O(1)	85.69(6)	N(1)–Ni(1)–N(30)	88.26(13)
N(2)–Co(1)–N(3A)	95.34(8)	N(2)–Co(1)–N(3A)	94.73(5)	N(2)–Ni(1)–N(3A)	93.92(13)
N(2)–Co(1)–N(4A)	169.68(8)	N(2)–Co(1)–N(4A)	168.69(6)	N(2)–Ni(1)–N(4A)	169.91(13)
N(2)–Co(1)–N(20)	91.29(9)	N(2)–Co(1)–N(20)	95.29(6)	N(2)–Ni(1)–N(20)	90.00(13)
N(2)–Co(1)–O(1)	90.78(9)	N(2)–Co(1)–O(1)	93.18(6)	N(2)–Ni(1)–N(30)	93.51(13)
N(3A)–Co(1)–N(4A)	74.57(8)	N(3A)–Co(1)–N(4A)	74.62(5)	N(3A)–Ni(1)–N(4A)	76.22(12)
N(3A)–Co(1)–N(20)	87.50(9)	N(3A)–Co(1)–N(20)	91.39(6)	N(3A)–Ni(1)–N(20)	91.63(13)
N(3A)–Co(1)–O(1)	91.92(9)	N(3A)–Co(1)–O(1)	96.16(6)	N(3A)–Ni(1)–N(30)	90.73(13)
N(4A)–Co(1)–N(20)	90.44(8)	N(4A)–Co(1)–N(20)	88.87(5)	N(4A)–Ni(1)–N(20)	88.20(13)
N(4A)–Co(1)–O(1)	87.46(8)	N(4A)–Co(1)–O(1)	84.37(6)	N(4A)–Ni(1)–N(30)	88.79(13)
N(20)–Co(1)–O(1)	177.89(9)	N(20)–Co(1)–O(1)	168.15(6)	N(20)–Ni(1)–N(30)	175.63(13)
Co(1)–N(2)–N(3)	132.27(16)	Co(1)–N(2)–N(3)	132.26(11)	Ni(1)–N(2)–N(3)	133.5(2)
N(2)–N(3)–Co(1A)	132.38(16)	N(2)–N(3)–Co(1A)	132.97(11)	N(2)–N(3)–Ni(1A)	132.6(2)

copper(II) complex incorporating a 4-substituted 3,5-di(2-pyridyl)-4*H*-1,2,4-triazole, $[Cu^{II}_2(NH_2dpt)(H_2O)_2(SO_4)_2] \cdot H_2O$.[20] It should be pointed out, however, that due to the fact that $[Cu^{II}_2(NH_2dpt)(H_2O)_2(SO_4)_2] \cdot H_2O$ features the dinuclear N',N^1,N^2,N'' single bridging coordination mode with an additional bridging sulfato co-ligand rather than the $(N',N^1,N^2,N'')_2$ double bridging coordination mode, the geometrical parameters of the two complexes cannot really be compared directly. The Cu–N_{pyr} bond lengths in complex **3** vary over the range 2.068(3)–2.079(3) Å. The Cu–N_{trz} bond lengths are shorter, as can be expected from the realisation of the $(N',N^1,N^2,N'')_2$ double bridging coordination mode,[2] and are in the range of 1.961(3)–1.972(3) Å. As in the other dinuclear 2:2 complexes of ibdpt described

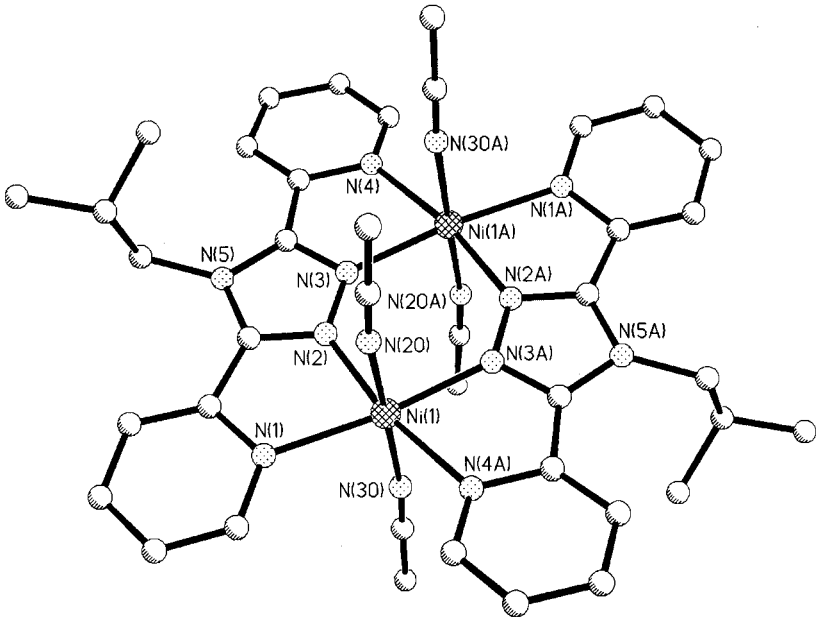

Figure 3. View of the molecular structure of the cation of $[Ni^{II}_2(ibdpt)_2(MeCN)_4](ClO_4)_4$ (**2**). Hydrogen atoms have been omitted for clarity. Symmetry operation used to generate equivalent atoms: (A) $-x + 1.5, -y + 0.5, -z + 1$.

Table 4. Selected angles [°] for $[Cu^{II}_2(ibdpt)_2(MeCN)_2(ClO_4)_2](ClO_4)_2 \cdot 2MeCN$ (**3**) and $[Cu^{II}(ibdpt)_2(ClO_4)_2]$ (**4**).

3				**4**	
N(1)–Cu(1)–N(2)	78.27(14)	N(6)–Cu(2)–N(7)	78.87(13)	N(1)–Cu(1)–N(2)	79.84(10)
N(1)–Cu(1)–N(3A)	169.46(14)	N(6)–Cu(2)–N(8B)	166.52(14)	N(1)–Cu(1)–N(1A)	180
N(1)–Cu(1)–N(4A)	111.21(13)	N(6)–Cu(2)–N(9B)	110.36(13)	N(1)–Cu(1)–N(2A)	100.16(10)
N(1)–Cu(1)–N(50)	86.75(15)	N(6)–Cu(2)–N(60)	96.57(13)	N(1)–Cu(1)–O(11)	89.13(9)
N(1)–Cu(1)–O(11)	89.83(12)	N(6)–Cu(2)–O(21)	84.54(11)	N(1)–Cu(1)–O(11A)	90.87(9)
N(2)–Cu(1)–N(3A)	92.70(14)	N(7)–Cu(2)–N(8B)	92.08(13)	N(2)–Cu(1)–N(2A)	180
N(2)–Cu(1)–N(4A)	169.92(13)	N(7)–Cu(2)–N(9B)	170.68(13)	N(2)–Cu(1)–O(11)	90.44(10)
N(2)–Cu(1)–N(50)	90.07(16)	N(7)–Cu(2)–N(60)	89.15(14)	N(2)–Cu(1)–O(11A)	89.56(10)
N(2)–Cu(1)–O(11)	96.85(13)	N(7)–Cu(2)–O(21)	86.69(12)	O(11)–Cu(1)–O(11A)	180
N(3A)–Cu(1)–N(4A)	78.17(13)	N(8B)–Cu(2)–N(9B)	78.61(13)		
N(3A)–Cu(1)–N(50)	98.81(16)	N(8B)–Cu(2)–N(60)	93.23(13)		
N(3A)–Cu(1)–O(11)	85.82(13)	N(8B)–Cu(2)–O(21)	84.98(11)		
N(4A)–Cu(1)–N(50)	87.17(15)	N(9B)–Cu(2)–N(60)	91.00(13)		
N(4A)–Cu(1)–O(11)	86.83(12)	N(9B)–Cu(2)–O(21)	92.80(11)		
N(50)–Cu(1)–O(11)	171.51(16)	N(60)–Cu(2)–O(21)	175.40(12)		
Cu(1)–N(2)–N(3)	133.5(3)	Cu(2)–N(7)–N(8)	134.0(3)		
N(2)–N(3)–Cu(1A)	133.8(3)	N(7)–N(8)–Cu(2B)	133.6(3)		

above, the pyridine–triazole–pyridine moieties of the ligands are not planar but show some doming and the torsion angles between the mean planes of the pyridine rings and the central triazole rings vary over the range 6.9(2)–9.0(2)°.

The overall architecture of $[Cu^{II}(ibdpt)_2(ClO_4)_2]$ (**4**) (Figure 5) is practically identical to that of $[Cu^{II}(pyppt)_2(ClO_4)_2] \cdot MeCN$ [pyppt = 3-phenyl-5-(2-pyridyl)-4-(4-pyridyl)-4*H*-1,2,4-triazole].[31] As a result of the realisation of the *trans*-$(N',N^1)_2$ coordination mode longer $Cu–N_{pyr}$ bond lengths [2.038(3) Å] than $Cu–N_{trz}$ bond lengths [1.962(3) Å] are observed in complex **4** (Table 2 and Table 4). The respective values are in good agreement with the corresponding bond lengths observed in $[Cu^{II}(pyppt)_2(ClO_4)_2] \cdot MeCN$ [2.045(2) and 1.989(2) Å, respectively]. This is also true for the Cu–O bond length which is 2.471(2) Å in complex **4** and 2.466(3) Å in $[Cu^{II}(pyppt)_2(ClO_4)_2] \cdot MeCN$.[31] The nitrogen atom of the non-coordinated pyridine ring points outwards towards the isobutyl group and the pyridine–triazole–pyridine moiety is almost perfectly planar, with the angles between the mean planes of the coordinated and the non-coordinated pyridine rings relative to the triazole mean plane being very small and identical within experimental error [2.0(2) and 1.9(2)°, respectively].

Magnetic Studies

The curves for the temperature dependence of the molar magnetic susceptibility and the effective magnetic moment for the dinuclear cobalt(II) complex **5** are shown in Figure S5 (Supporting Information). The maximum in susceptibility observed at 18 K (χ_m = 0.05383 $cm^3 mol^{-1}$) is due

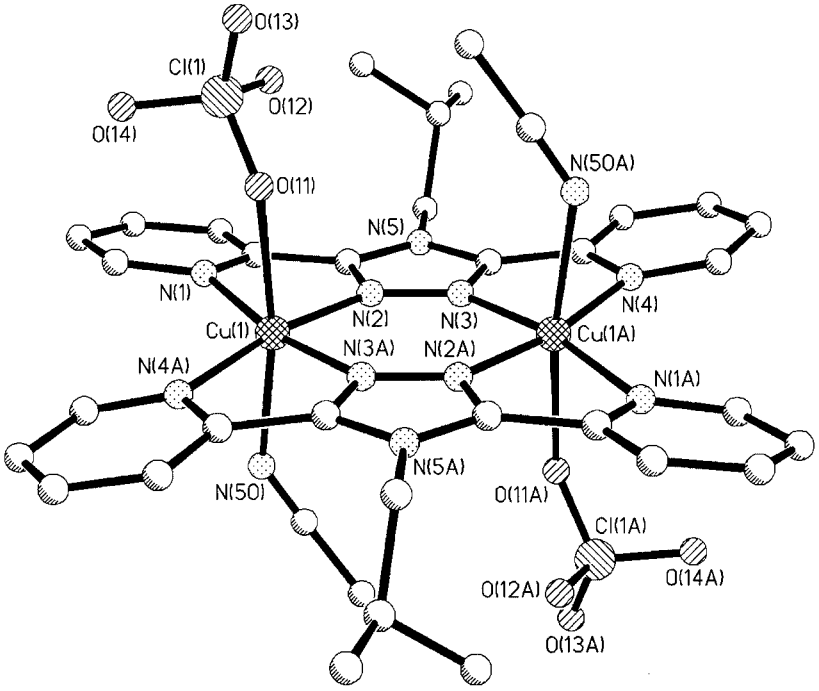

Figure 4. View of the molecular structure of one of the two crystallographically independent cations of $[Cu^{II}_2(ibdpt)_2(MeCN)_2(ClO_4)_2](ClO_4)_2 \cdot 2MeCN$ (**3**). Hydrogen atoms have been omitted for clarity. Symmetry operation used to generate equivalent atoms: (A) $-x + 1, -y, -z + 2$.

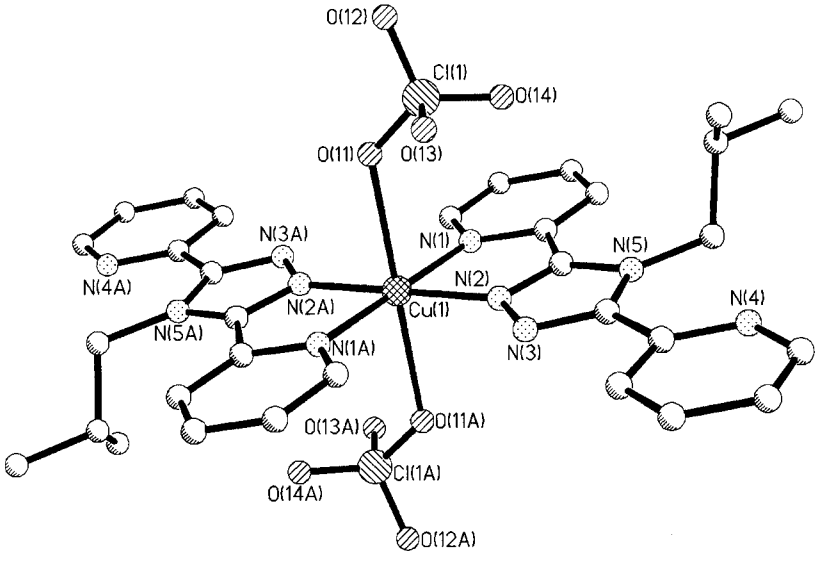

Figure 5. View of the molecular structure of $[Cu^{II}(ibdpt)_2(ClO_4)_2]$ (**4**). Hydrogen atoms have been omitted for clarity. Symmetry operation used to generate equivalent atoms: (A) $-x + 2, -y, -z + 2$.

to antiferromagnetic coupling across the two 1,2,4-triazole bridges. The corresponding magnetic moment data show a μ_{eff} value of 4.64 μ_B at room temperature which is a little reduced from typical weak-field octahedral cobalt(II) centres having $^4T_{1g}$ (d^7) ground states. Low symmetry ligand field effects, combined with spin-orbit coupling, cause splitting of these single-ion states and thus allow for the use of the Heisenberg–Van Vleck exchange Hamiltonian ($-2J\mathbf{S_1 \cdot S_2}$) for an $S = 3/2$ dimer as a reasonable approximation for fitting the data. A good fit was obtained using the parameters $J = -3.76$ cm^{-1}, $g = 2.45$, $TIP = 0$ cm^3 mol^{-1} and 0.2% monomer (in this and in all other cases all parameters were allowed to vary for the best fit except for *TIP* which was fixed). The high g value accounts for spin-orbit and orbital degeneracy effects. The value of J is similar to that obtained for related compounds incorporating NH_2dpt[19] and is somewhat less than observed for pyridazine-bridged systems.[32,33]

The dinuclear nickel(II) complex **6** also exhibits antiferromagnetic coupling. The fitted curve for the molar magnetic

susceptibility reaches a maximum at 38 K (χ_m = 0.01142 $cm^3 mol^{-1}$) and the corresponding effective magnetic moment decreases from 2.81 μ_B at room temperature to 0.17 μ_B at 4.2 K (Figure S6, Supporting Information). The data were fitted extremely well to an $S = 1$ dimer–$2J\mathbf{S_1}\cdot\mathbf{S_2}$ model using $J = -13.0\ cm^{-1}$, $g = 2.08$, $TIP = 85\times10^{-6}\ cm^3 mol^{-1}$ and 0.3% monomer. The coupling is slightly stronger than that found in related doubly 1,2,4-triazole-bridged complexes incorporating NH_2dpt[19] but weaker than in doubly pyridazine-bridged derivatives ($J \approx -21\ cm^{-1}$).[33]

The analogous dinuclear copper(II) complex **7** shows quite strong antiferromagnetic coupling. Thus, the maximum in molar magnetic susceptibility is observed at 185 K (χ_m = 0.00093 $cm^3 mol^{-1}$) and the corresponding effective magnetic moment decreases from 1.39 μ_B at room temperature to 0.22 μ_B at 4.2 K (Figure 6). Monomer impurity is clearly evident in the susceptibility plot below ca. 50 K. Fitting to the Bleaney–Bowers $S = 1/2$ dimer model[34] yielded $J = -105\ cm^{-1}$, $g = 1.87$, $TIP = 60\times10^{-6}\ cm^3 mol^{-1}$ and 1.5% monomer. The g value is lower than expected for a tetragonally elongated copper(II) site which is probably due to the loss of the remaining MeCN solvate affecting the molar mass used in the calculation of the molar magnetic susceptibilities. The strong antiferromagnetic coupling is compatible with the triazole p orbitals of the two 1,2,4-triazole nitrogen donors coupling effectively with the $d(x^2–y^2)$ magnetic orbitals of the copper(II) centres within the planar six-membered $(Cu–N_{trz}–N_{trz})_2$ ring. Other doubly 1,2,4-triazole-bridged compounds with symmetrical bis(bidentate) ligands[35–37] have similar values of J while weaker coupling is found in systems incorporating the unsymmetrical anionic 3-(2-pyridyl)-1,2,4-triazolato ligand ($J \approx -50\ cm^{-1}$).[38,39] Interestingly, in $[Cu^{II}_2(NH_2dpt)(H_2O)_2(SO_4)_2]\cdot H_2O$,[20] containing a single 1,2,4-triazole bridge and an additional bridging sulfato co-ligand between the two copper(II) centres, the J value was found to be $-34.5\ cm^{-1}$, i. e. about one third of the value obtained here for the doubly 1,2,4-triazole-bridged system. Clearly, the poor superexchange pathway provided by a bidentate sulfate ion in combination with only one 1,2,4-triazole pathway leads to the diminution in J. The Cu···Cu separation in the present complex is significantly shorter than in the singly 1,2,4-triazole-bridged complex $[Cu^{II}_2(NH_2dpt)(H_2O)_2(SO_4)_2]\cdot H_2O$.[20] The $Cu–N_{trz}–N_{trz}$ angles of ca. 133–134° in the present complex are somewhat smaller than the corresponding angles of ca. 136–138° found in the unsymmetrical singly 1,2,4-triazole-bridged example. Haasnoot and coworkers[39] have concluded that $Cu–N_{trz}–N_{trz}$ angles of ca. 134° in symmetrical doubly 1,2,4-triazole-bridged systems lead to the largest possible coupling with $J \approx -120\ cm^{-1}$. The J value of $-105\ cm^{-1}$ observed here is only a little smaller than the predicted value.

Conclusions

The new ligand ibdpt was used to investigate the coordination chemistry of a 4-alkyl-substituted 3,5-di(2-pyridyl)-4*H*-1,2,4-triazole for the first time. We initially focused on the exploration of the dinucleation behaviour of this ligand. It has been found that, unlike with 4-aryl-substituted 3,5-di(2-pyridyl)-4*H*-1,2,4-triazoles, dinuclear complexes can be readily obtained. This result clearly supports our hypothesis that whether or not dinuclear complexes of bis(bidentate) 4-substituted 3,5-di(2-pyridyl)-4*H*-1,2,4-triazoles can be formed is strongly influenced by the nature of the actual substituent on N^4, including its electronic effect on the 1,2,4-triazole ring. In the resulting dinuclear doubly 1,2,4-triazole-bridged complexes the two metal centres have been found to be antiferromagnetically coupled. In light of these findings the synthesis of exchange-coupled dinuclear iron(II) spin crossover compounds of ibdpt and other 4-alkyl-3,5-di(2-pyridyl)-4*H*-1,2,4-triazoles[30] appears possible. Studies in this direction are currently underway and will be reported in due course.[16]

Experimental Section

General Remarks: All solvents used were laboratory reagent grade. $Co(ClO_4)_2\cdot 6H_2O$, $Ni(ClO_4)_2\cdot 6H_2O$ and $Cu(ClO_4)_2\cdot 6H_2O$ were purchased from Aldrich and used as received. 4-Isobutyl-3,5-di(2-pyridyl)-4*H*-1,2,4-triazole (ibdpt) was prepared as described elsewhere.[22,30] Elemental analyses were carried out by the Campbell Microanalytical Laboratory at the University of Otago. Infrared spectra were recorded over the range 4000–400 cm^{-1} with a Perkin–Elmer Spectrum BX FT-IR spectrophotometer. ESI mass spectra were run with a MicroMass LCT mass spectrometer at the University of Canterbury. X-ray data were collected with a Bruker SMART CCD area detector using graphite-monochromated Mo-K_α radiation (λ = 0.71073 Å). The structures were solved by direct methods with SIR-92[40] and refined against F^2 using all data by full-matrix least-squares techniques with SHELXL-97.[41] Magnetic data were recorded over the range 300–4.2 K with a Quantum Design MPMS5 SQUID magnetometer with an applied field of 1 T.

Caution: While no problems were encountered in the course of this work, ClO_4^- salts are potentially explosive and should be handled with appropriate care!

$[Co^{II}_2(ibdpt)_2(MeCN)_2(H_2O)_2](ClO_4)_4$ (1) and $Co^{II}_2(ibdpt)_2(ClO_4)_4(MeCN)(H_2O)$ (5): An orange solution of $Co(ClO_4)_2\cdot 6H_2O$ (366 mg, 1.00 mmol) in MeCN (5 mL) was added to a colourless solution of ibdpt (279 mg, 1.00 mmol) in MeCN (35 mL). The resulting orange solution was stirred at room temperature for 2 hours before it was subjected to vapour diffusion of Et_2O. This afforded crystalline $[Co^{II}_2(ibdpt)_2(MeCN)_2(H_2O)_2](ClO_4)_4$ (**1**) as a mixture of the red-orange polymorph **1a** and the yellow-orange polymorph **1b** which were both identified by X-ray diffraction. The ratio of the two crystal types was variable and they both readily lost solvent when taken out of their mother liquor which in the case of the yellow-orange polymorph **1b** was accompanied by a colour change to red-orange while no colour change was observed for the red-orange polymorph **1a**. A bulk sample of complex **1** was dried in vacuo to give 541 mg (95%) of $Co^{II}_2(ibdpt)_2(ClO_4)_4(MeCN)(H_2O)$ (**5**) as dull red-orange crystals. This material was used for further characterisation and magnetic studies. $C_{34}H_{39}Cl_4Co_2N_{11}O_{17}$ (1133.43): calcd. C 36.03, H 3.47, N 13.59; found C 35.81, H 3.56, N 13.66. IR (KBr): $\tilde{\nu}$ = 3374, 2966, 1607, 1579, 1511, 1498, 1467, 1436, 1394, 1299, 1280, 1248, 1145, 1117, 1083, 1027, 1002, 940, 928, 793, 760, 744, 709, 688, 668, 636, 626, 515, 417 cm^{-1}. ESI-

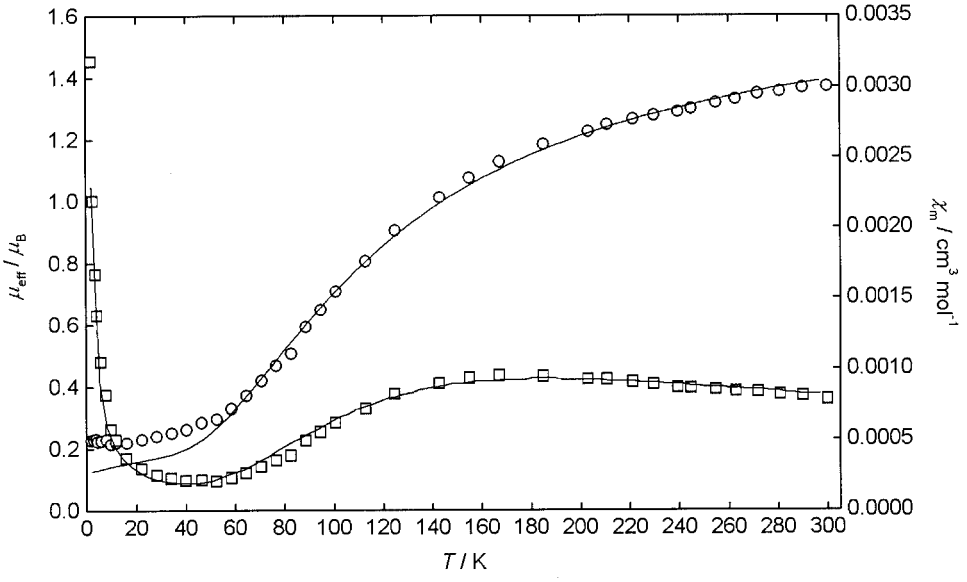

Figure 6. Temperature dependence of the effective magnetic moment μ_{eff} (○) and the molar magnetic susceptibility χ_m (□) per copper centre for $Cu^{II}_2(ibdpt)_2(ClO_4)_4(MeCN)$ (**7**). The solid line represents the best fit: $J = -105\ cm^{-1}$, $g = 1.87$, $TIP = 60 \times 10^{-6}\ cm^3 mol^{-1}$, 1.5% monomer.

MS (pos., MeCN): *m*/*z* = 308.6 $[Co(ibdpt)_2]^{2+}$, 329.1 $[Co(ibdpt)_2(MeCN)]^{2+}$, 448.2 $[Co(ibdpt)_3]^{2+}$, 478.1 $[Co(ibdpt)(MeCN)(ClO_4)]^+$, 716.2 $[Co(ibdpt)_2(ClO_4)]^+$, 973.0 $[Co_2(ibdpt)_2(ClO_4)_3]^+$, 995.4 $[Co(ibdpt)_3(ClO_4)]^+$, 1254.2 $[Co_2(ibdpt)_3(ClO_4)_3]^+$, 1531.5 $[Co_2(ibdpt)_4(ClO_4)_3]^+$.

$[Ni^{II}_2(ibdpt)_2(MeCN)_4](ClO_4)_4$ (2) and $Ni^{II}_2(ibdpt)_2(ClO_4)_4(MeCN)$ (6): A blue solution of $Ni(ClO_4)_2{\cdot}6H_2O$ (366 mg, 1.00 mmol) in MeCN (5 mL) was added to a colourless solution of ibdpt (279 mg, 1.00 mmol) in MeCN (35 mL). The resulting purple solution was stirred at room temperature for 2 hours before it was subjected to vapour diffusion of Et_2O. This afforded $[Ni^{II}_2(ibdpt)_2(MeCN)_4](ClO_4)_4$ (**2**) as purple crystals which were identified by X-ray diffraction. The crystals readily lost solvent when taken out of their mother liquor. A bulk sample of complex **2** was dried in vacuo to yield 547 mg (98%) of $Ni^{II}_2(ibdpt)_2(ClO_4)_4(MeCN)$ (**6**) as dull purple crystals. This material was used for further characterisation and magnetic studies. $C_{34}H_{37}Cl_4N_{11}Ni_2O_{16}$ (1114.92): calcd. C 36.63, H 3.34, N 13.82; found C 36.30, H 3.56, N 14.16. IR (KBr): $\tilde{\nu}$ = 3334, 2967, 1606, 1577, 1510, 1465, 1437, 1397, 1379, 1283, 1245, 1145, 1118, 1082, 1032, 1000, 940, 929, 791, 756, 710, 686, 668, 636, 626, 514, 418 cm^{-1}. ESI-MS (pos., MeCN): *m*/*z* = 308.1 $[Ni(ibdpt)_2]^{2+}$, 328.7 $[Ni(ibdpt)_2(MeCN)]^{2+}$, 447.7 $[Ni(ibdpt)_3]^{2+}$, 477.1 $[Ni(ibdpt)(MeCN)(ClO_4)]^+$, 715.2 $[Ni(ibdpt)_2(ClO_4)]^+$, 975.0 $[Ni_2(ibdpt)_2(ClO_4)_3]^+$, 994.4 $[Ni(ibdpt)_3(ClO_4)]^+$, 1252.2 $[Ni_2(ibdpt)_3(ClO_4)_3]^+$, 1533.5 $[Ni_2(ibdpt)_4(ClO_4)_3]^+$.

$[Cu^{II}_2(ibdpt)_2(MeCN)_2(ClO_4)_2](ClO_4)_2{\cdot}2MeCN$ (3) and $Cu^{II}_2(ibdpt)_2(ClO_4)_4(MeCN)$ (7): A blue solution of $Cu(ClO_4)_2{\cdot}6H_2O$ (371 mg, 1.00 mmol) in MeCN (5 mL) was added to a colourless solution of ibdpt (279 mg, 1.00 mmol) in MeCN (35 mL). The resulting blue solution was stirred at room temperature for 2 hours before it was subjected to vapour diffusion of Et_2O. This afforded $[Cu^{II}_2(ibdpt)_2(MeCN)_2(ClO_4)_2](ClO_4)_2{\cdot}2MeCN$ (**3**) as blue-green crystals along with a small amount of $[Cu^{II}(ibdpt)_2(ClO_4)_2]$ (**4**) as steel-blue crystals which were both identified by X-ray diffraction. The crystals of complex **3** readily lost solvent when taken out of their mother liquor. A bulk sample of complex **3** was dried in vacuo to give 485 mg (86%) of $Cu^{II}_2(ibdpt)_2(ClO_4)_4(MeCN)$ (**7**) as dull blue-green crystals. This material was used for further characterisation and magnetic studies. $C_{34}H_{37}Cl_4Cu_2N_{11}O_{16}$ (1124.64): calcd. C 36.31, H 3.32, N 13.70; found C 36.53, H 3.24, N 13.73. IR (KBr): $\tilde{\nu}$ = 3454, 2967, 1614, 1586, 1514, 1472, 1442, 1398, 1378, 1280, 1254, 1144, 1119, 1087, 1014, 929, 793, 763, 746, 710, 688, 667, 624, 507, 417 cm^{-1}. ESI-MS (pos., MeCN): *m*/*z* = 310.6 $[Cu(ibdpt)_2]^{2+}$, 331.1 $[Cu(ibdpt)_2(MeCN)]^{2+}$, 450.2 $[Cu(ibdpt)_3]^{2+}$, 482.1 $[Cu(ibdpt)(MeCN)(ClO_4)]^+$, 720.2 $[Cu(ibdpt)_2(ClO_4)]^+$, 983.0 $[Cu_2\text{-}(ibdpt)_2(ClO_4)_3]^+$, 1262.2 $[Cu_2(ibdpt)_3(ClO_4)_3]^+$, 1541.3 $[Cu_2\text{-}(ibdpt)_4(ClO_4)_3]^+$.

$[Cu^{II}(ibdpt)_2(ClO_4)_2]$ (4): A blue solution of $Cu(ClO_4)_2{\cdot}6H_2O$ (185 mg, 0.50 mmol) in MeCN (5 mL) was added to a colourless solution of ibdpt (279 mg, 1.00 mmol) in MeCN (5 mL). The resulting blue solution was stirred at room temperature for 24 hours during which time a precipitate formed. The solid was filtered off and washed with small amount of MeCN. Drying in vacuo gave 198 mg (48%) of $[Cu^{II}(ibdpt)_2(ClO_4)_2]$ (**4**) as a pale blue powder. $C_{32}H_{34}Cl_2CuN_{10}O_8$ (821.14): calcd. C 46.81, H 4.17, N 17.06; found C 46.64, H 4.10, N 16.98. IR (KBr): $\tilde{\nu}$ = 3447, 2971, 1612, 1584, 1497, 1460, 1428, 1395, 1310, 1280, 1247, 1171, 1131, 1054, 1021, 926, 796, 762, 751, 739, 712, 693, 668, 649, 623, 592 cm^{-1}. ESI-MS (pos., MeCN): *m*/*z* = 310.6 $[Cu(ibdpt)_2]^{2+}$, 383.1 $[Cu(ibdpt)(MeCN)]^+$, 621.2. $[Cu(ibdpt)_2]^+$, 785.1 $[Cu_2(ibdpt)_2(ClO_4)]^+$, 900.5 $[Cu(ibdpt)_3]^+$, 1064.3 $[Cu_2(ibdpt)_3(ClO_4)]^+$. Vapour diffusion of Et_2O into the mother liquor or a solution of the powder in MeCN gave steel-blue crystals of $[Cu^{II}(ibdpt)_2(ClO_4)_2]$ (**4**) which were identified by X-ray diffraction.

X-ray Crystallography: All non-hydrogen atoms, except N(90) to C(91) of the disordered MeCN solvate in complex **3**, were refined anistropically. All hydrogen atoms, except H(101) and H(102) of the axial H_2O co-ligands in complexes **1a** and **1b**, were placed at calculated positions using a riding model with thermal parameters 1.2 times the equivalent isotropic thermal parameters of the atom to which they were bonded. The hydrogen atoms of the H_2O co-ligands in complexes **1a** and **1b** were located from the difference maps and allowed to refine freely. In the structure of complex **2** one of the two methyl groups of the isobutyl moiety was disordered

over two positions with site occupancy factors of 0.75 and 0.25 for C(17) and C(17′), respectively. One of the ClO_4^- ions was also disordered over two positions with a site occupancy factor of 0.50 for both Cl(2) to O(24) and Cl(3) to O(34). The structure of complex **3** featured two crystallographically independent moieties within the asymmetric unit. In one of the ClO_4^- ions three of the oxygen atoms were disordered over two positions with a site occupancy factor of 0.50 for both O(42) to O(44) and O(42′) to O(44′). One of the MeCN solvates was also disordered over two positions with site occupancy factors of 0.75 for N(80) to C(81) and 0.25 for N(90) to C(91). CCDC-250036 (**1a**), -250037 (**1b**), -250038 (**2**), -250039 (**3**) and -250040 (**4**) contain the supplementary crystallographic data for this paper. These data can be obtained free of charge from The Cambridge Crystallographic Data Centre via www.ccdc.cam.ac.uk/data_request/cif.

Supporting Information (see also the footnote on the first page of this article): A PDF file (five pages) with Supporting Information for this article is available on the internet under http://www.eurjic.org or from the authors. The file contains a view of the molecular structure of complex **1b** (Figure S1), an overlay of the molecular structures of complexes **1a** and **1b** (Figure S2), illustrations of the hydrogen bonding in complexes **1a** and **1b** (Figures S3 and S4, respectively) and the curves for the molar magnetic susceptibilities and effective magnetic moments of complexes **5** and **6** over the range 300–4.2 K (Figures S5 and S6, respectively).

Acknowledgments

This work was supported by a number of grants from the University of Otago (including a University of Otago Postgraduate Scholarship to MHK and a Bridging Grant) and the Australian Research Council (Discovery Grant). Mr. B. M. Clark (University of Canterbury) is thanked for running the ESI mass spectra and Dr. J. Hausmann (University of Otago) for helpful discussions. SB is grateful for the provision of sabbatical leave which has facilitated the completion of this manuscript and thanks her host Prof. A. K. Powell (University of Karlsruhe) for helpful discussions and the DFG Research Center for Functional Nanostructures (CFN) for the award of a Visiting Professorship.

[1] J. G. Haasnoot, *Coord. Chem. Rev.* **2000**, *200–202*, 131–185.
[2] M. H. Klingele, S. Brooker, *Coord. Chem. Rev.* **2003**, *241*, 119–132.
[3] U. Beckmann, S. Brooker, *Coord. Chem. Rev.* **2003**, *245*, 17–29.
[4] O. Kahn, E. Codjovi, *Phil. Trans. R. Soc. Lond. A* **1996**, *354*, 359–379.
[5] J. G. Haasnoot, in: *Magnetism: A Supramolecular Function* (Ed.: O. Kahn), Kluwer, Dordrecht, **1996**, pp. 299–321.
[6] L. G. Lavrenova, S. V. Larionov, *Koord. Khim.* **1998**, *24*, 403–420; *Russ. J. Coord. Chem.* **1998**, *24*, 379–395.
[7] P. J. van Koningsbruggen, *Top. Curr. Chem.* **2004**, *233*, 123–149.
[8] O. Kahn, J. P. Launay, *Chemtronics* **1988**, *3*, 140–151.
[9] J. Zarembowitch, O. Kahn, *New. J. Chem.* **1991**, *15*, 181–190.
[10] O. Kahn, J. Kröber, C. Jay, *Adv. Mater.* **1992**, *4*, 718–728.
[11] O. Kahn, C. J. Martinez, *Science* **1998**, *279*, 44–48.
[12] J.-F. Létard, P. Guionneau, L. Goux-Capes, *Top. Curr. Chem.* **2004**, *235*, 221–249.
[13] O. Kahn, Y. Garcia, J. F. Létard, C. Mathonière, in: *Supramolecular Engineering of Synthetic Metallic Materials: Conductors and Magnets* (Eds.: J. Veciana, C. Rovira, D. B. Amabilino), Kluwer, Dordrecht, **1998**, pp. 127–144.
[14] J. A. Real, A. B. Gaspar, V. Niel, M. C. Muñoz, *Coord. Chem. Rev.* **2003**, *236*, 121–141.
[15] M. H. Klingele, B. Moubaraki, J. D. Cashion, K. S. Murray, S. Brooker, *Chem. Commun.* **2005**, in press [DOI: 10.1039/b415891a].
[16] C. D. Brandt, M. Weitzer, B. Moubaraki, K. S. Murray, S. Brooker, unpublished results.
[17] V. Ksenofontov, A. B. Gaspar, V. Niel, S. Reiman, J. A. Real, P. Gütlich, *Chem. Eur. J.* **2004**, *10*, 1291–1298.
[18] J. A. Real, A. B. Gaspar, M. C. Muñoz, P. Gütlich, V. Ksenofontov, H. Spiering, *Top. Curr. Chem.* **2004**, *233*, 167–193.
[19] F. J. Keij, R. A. G. de Graaff, J. G. Haasnoot, J. Reedijk, *J. Chem. Soc., Dalton Trans.* **1984**, 2093–2097.
[20] P. J. van Koningsbruggen, D. Gatteschi, R. A. G. de Graaff, J. G. Haasnoot, J. Reedijk, C. Zanchini, *Inorg. Chem.* **1995**, *34*, 5175–5182.
[21] S. K. Mandal, H. J. Clase, J. N. Bridson, S. Ray, *Inorg. Chim. Acta* **1993**, *209*, 1–4.
[22] M. H. Klingele, PhD Thesis, University of Otago (New Zealand), **2004**.
[23] M. H. Klingele, P. D. W. Boyd, B. Moubaraki, K. S. Murray, S. Brooker, manuscript in preparation.
[24] S.-C. Shao, D.-R. Zhu, X.-H. Zhu, X.-Z. You, S. S. S. Raj, H.-K. Fun, *Acta Crystallogr. Sect. C* **1999**, *55*, 1412–1413.
[25] S. C. Shao, D. R. Zhu, T. W. Wang, Y. Zhang, S. S. S. Raj, H.-K. Fun, *Chin. Chem. Lett.* **2000**, *11*, 93–94.
[26] D. Zhu, Y. Song, Y. Liu, Y. Xu, Y. Zhang, X. You, *Transition Met. Chem.* **2000**, *25*, 589–593.
[27] D.-R. Zhu, Y. Song, Y. Xu, Y. Zhang, S. S. S. Raj, H.-K. Fun, X.-Z. You, *Polyhedron* **2000**, *19*, 2019–2025.
[28] D. Zhu, Y. Xu, Y. Mei, Y. Shi, C. Tu, X. You, *J. Mol. Struct.* **2001**, *559*, 119–125.
[29] D. Zhu, Y. Xu, Z. Yu, Z. Guo, H. Sang, T. Liu, X. You, *Chem. Mater.* **2002**, *14*, 838–843.
[30] M. H. Klingele, S. Brooker, *Eur. J. Org. Chem.* **2004**, 3422–3434.
[31] M. H. Klingele, S. Brooker, *Inorg. Chim. Acta* **2004**, *357*, 3413–3417.
[32] S. Brooker, D. J. de Geest, R. J. Kelly, P. G. Plieger, B. Moubaraki, K. S. Murray, G. B. Jameson, *J. Chem. Soc. Dalton Trans.* **2002**, 2080–2087.
[33] Y. Lan, D. K. Kennepohl, B. Moubaraki, K. S. Murray, J. D. Cashion, G. B. Jameson, S. Brooker, *Chem. Eur. J.* **2003**, *9*, 3772–3784.
[34] B. Bleaney, K. D. Bowers, *Proc. R. Soc. Lond. A* **1952**, *214*, 451–465.
[35] R. Prins, P. J. M. W. L. Birker, J. G. Haasnoot, G. C. Verschoor, J. Reedijk, *Inorg. Chem.* **1985**, *24*, 4128–4133.
[36] W. M. E. Koomen-van Oudenniel, R. A. G. de Graaff, J. G. Haasnoot, R. Prins, J. Reedijk, *Inorg. Chem.* **1989**, *28*, 1128–1133.
[37] P. J. van Koningsbruggen, J. G. Haasnoot, R. A. G. de Graaff, J. Reedijk, S. Slingerland, *Acta Crystallogr. Sect. C* **1992**, *48*, 1923–1926.
[38] P. M. Slangen, P. J. van Koningsbruggen, J. G. Haasnoot, J. Jansen, S. Gorter, J. Reedijk, H. Kooijman, W. J. J. Smeets, A. L. Spek, *Inorg. Chim. Acta* **1993**, *212*, 289–301.
[39] P. M. Slangen, P. J. van Koningsbruggen, K. Goubitz, J. G. Haasnoot, J. Reedijk, *Inorg. Chem.* **1994**, *33*, 1121–1126.
[40] A. Altomare, G. Cascarano, C. Giacovazzo, A. Guagliardi, M. C. Burla, G. Polidori, M. Camalli, *J. Appl. Crystallogr.* **1994**, *27*, 435.
[41] G. M. Sheldrick, T. R. Schneider, *Methods Enzymol.* **1997**, *277*, 319–343.

Received: September 21, 2004